PCT

INTERNATIONAL APPLICATION PUBLISHED UNDER THE PATENT COOPERATION TREATY (PCT)

(54) Title: PREPARATION OF METAL OXIDE POWDERS USING ACTIVATED BALL MILLING

(57) Abstract

Total phase transformation of hematite to magnetite was accomplished at room temperature by wet magnetomechanical activation of hematite. Low energy mechanical activation of the oxide surface is sufficient to effect the transformation. Oxygen bonds on a α-Fe$_2$O$_3$ oxide surface are apparently broken during the mechanical activation process and oxygen is released (removed) to the dispersing polar liquid. The oxygen pressure during the process as well as the nature of the dispering liquid have a critical influence on successful and fast phase transformation. Thus, all preparation performed in air, dry conditions or with nonpolar or saturated hydrocarbons (benzene, anthracene) show that the process of hematite reduction is non existent or very slow. Normal air pressure and/or application of hydrocarbons suppress the transformation. The effects of prolonged milling in air and vacuum on BaFe$_{12}$O$_{19}$ ionic crystal structure and particle morphology have been analysed. X-ray diffraction, scanning electron microscopy and thermal analysis experiments show, that for vacuum milled material, the ordered structure transforms progressively into a stable disordered nanocrystalline phase. For air milled samples, apart from a structural transformation, chemical decomposition was found. Application of heat treatment restores perfect Ba-ferrite crystal structure with the particle remaining in the submicron size range. With structural changes during annealing, the magnetic properties were altered. Radically different hysteresis behaviour was obtained for powders annealed at 1273 K. The value of volume magnetisation $4\pi M_s$ = 335.4 - 347.2 kA/m is near the value for premilled ferrite powder (10 % lower), but measured coercivity value H_c = 393.9 - 445.6 kA/m was improved quite remarkably by a factor of 6 due to the fine crystalline grain structure.

PREPARATION OF METAL OXIDE POWDERS USING ACTIVATED BALL MILLING

Background of the Invention

5   The present invention relates to new preparation technique concerns production of magnetic powder.

In a first aspect, the present invention provides methods of improving the magnetic coercivity of a product. In particular, the present invention relates to a method

10   of improving the magnet coercivity in a magnetic oxide, and more particularly, in a hexagonal system ferrite powder.

In a second aspect, the present invention relates to methods of reduction of hematite (Fe_2O_3) and producing magnetite (Fe_3O_4) powder. The reduction method of the

15   invention is based on combination of mechanical and a chemical activation processes, both performed in the same time and near room temperature.

Both methods of producing magnetic powders from oxides rely on controlled activated ball milling.

20

Description of the Prior Art

Mechanical treatment of simple and complex iron oxides has become extremely important in many technological processes for production of electronic components during the last few decades. Low cost, iron-oxide-based magnetic ceramic materials

25   play a most important role in memory devices as well as magnetic recording media. The overall magnetic properties of these materials are governed by a complex combination of intrinsic and extrinsic behaviour. An intrinsic property such as saturation magnetisation is determined by material composition, whereas an extrinsic property such as magnetic coercivity is, to a large extent, determined by the microstructure which is,

30   in turn, influenced strongly by the processing procedures. Barium ferrite $BaFe_{12}O_{19}$ and its variety of chemical modifications (possible cationic substitution) are well known typical complex oxide compounds widely used in production of ceramic hard magnets and magnetic inks for high density recording. Three decades ago, the first studies to

- 2 -

improve the magnetic properties with optimised mechanical and thermal treatment were performed. Up to this time all investigations reports describe improvements in 'classical' ceramic methods in which premilled components (oxides and/or carbonates) were thermally treated: calcinated to yield the final crystalline product. As a result of

5   decreased particle size of the solid reactants before heat treatment, the calcination was influenced, and the lowering of synthesis temperature with shorter annealing time was obtained. This technological progress mainly affected the final size of the crystal grains due to fast diffusion between fine powder particles of reacting compounds, thus, achieving the required barium ferrite stoichiometry within a very small volume. With

10   magnetisation remaining rather constant, the value of coercive field increases as the size of crystal grains decreases. However, by using high temperatures the crystals grain size are often with the size exceeds 10 μm up to 100 μm. Such particles, well above single-domain critical size (single domain size is ~1 μm at room temperature for pure barium ferrite) are to large for specific applications. These particles are excluded from

15   applications in memory media where the typical active layer is 2 - 3 μm thick and the particle size has to be in the submicron range 0.1 - 0.5 μm. In recent times many different chemical routes have been proposed and investigations dealing with mechanical processing were nearly forgotten completely. On the other hand, the first ball milling experiments were simple and concerned wet or dry grinding processes, dealing mainly

20   with grinding of components for further synthesis. Only a few research groups were using barium ferrite as a starting material, and investigating influence of milling time on crystal structure and magnetic properties. Simple milling devices were used and all these studies suffered from lack of control over milling conditions. While the nature of mechanochemical reactions involving nonmetallics has advanced somewhat, the

25   fundamental processes governing the evolution of structure, the kinetics. and thermodynamics of resulting chemical or physical transformation remain misunderstood. Their elucidation requires more empirical studies. The aim of the first part of the present study is to further exploit improved understanding of the milling process, its influence on changes in solid surface morphology and distinguish between solid state reactions

30   either at the surface or in the bulk. Additionally, along with structural changes, we investigate the influence of heat treatment on the particle morphology, structure and magnetic properties in relation to preparation routes i.e. air and vacuum milling. The example given hereinafter pertains to barium ferrite and improved magnetic coercivity

- 3 -

therefor which can be realised under controlled activated milling.

Relevant to the second method outlined in this invention, is that there are many reviews outlining mechanochemical reactions occuring during ball milling. Milling is

5   a highly active mechanical process which consists of grinding through impact, compression and attrition. The strain, shear, thermal and kinetic energy transforms all the solids involved from one phase or compound into another through polymorphic or solid state reactions. The process can be performed in different gas pressure, temperature and in dry or wet (different dispersing agents) conditions. In polymorphic

10 transformations the transition can take place from metastable to stable phases and vice versa, with possible binary coexistence in steady state equilibrium, depending on the mechanical treatment regime and conditions. In the recent developments in ball milling techniques one central fundamental problem remains unanswered: Is there a phenomenology capable of predicting which milling conditions to select to achieve an

15 a priori chosen structure or microstructure? Attempts at both experimental and theoretical classification have been made. The matter is complex, results often appear mysterious and it is well accepted that various physical and chemical mechanisms occurring in material processing can be quite different even for structurally similar compounds.

20

The second method of the present study concerns phase transitions in simple iron oxides, in particular the hematite - magnetite transformation. Preparation and properties or iron oxides have been the subject of numerous studies because of their importance in magnetic materials technology. A schematic diagram of the whole process is presented

25 below (see Fig. 1), where arrows represent chemical solid state reactions: oxidation or reduction (typically achieved by the use of hydrogen at high temperature). Of concern here are the phase magnetite, (Fe_3O_4) maghemite (γ-Fe_2O_3) and hematite (α-Fe_2O_3) that are "central" in this diagram. Phase transformations and reactions of Fe_2O_3 during grinding were extensively studied during the last two decades.

30

The formation of γ-Fe_2O_3 from α-Fe_2O_3 via grinding would present some very interesting questions from a thermodynamic point of view. However, according to early experiments only the reverse reaction can be accomplished. Even on milling of α-Fe_2O_3

- 4 -

in pure hydrogen atmosphere a direct production of γ phase does not seem possible.

Another attempt at mechanchemical reduction concerns the hematite - magnetite transformation. All experiments in this area were performed by application of high energy ball milling (normally vibratory ball mixer/mills) and an oxygen free atmosphere. The results always show that a mixture of iron oxides is produced due to extensive wear of the iron containing mill and the grinding balls. Prolonged very high energy milling (7 hours) in this process results in the detection of Fe, FeO and Fe_3O_4 mainly because of the reaction between hematite and iron from the mill material. Similar complex mixtures of oxides were obtained for hematite milled for 70 hours with graphite as a reducing agent, and the same problem with contamination from the vial and balls was observed.

Finally, as background to the present study we have to mention the temperature versus oxygen pressure $(T - PO_2)$ phase diagram of the iron-oxide system, which is presented below in Fig. 2. As can be seen the stability range of α-Fe_2O_3 corresponds to a wide range of oxygen pressure. However, is well known from temperatures vs. composition phase diagram that in contrast to wustite or magnetite, hematite exhibits a very small deviation from stoichiometry and only at high temperature (above 900 K). Taking this into account, the formation of multiphase material in oxygen free and high energy milling can be explained by effects due to the wide energy dispersion during ball milling. In fact the ball movement can not be controlled and is more or less chaotic, as is the ratio between shear and kinetic energy. Thus, conventional milling does not product a single oxide phase. However, it is the major outcome of this invention that we have produced for the first time the complete transformation of hematite to magnetite under activated, controlled ball milling.

Ball milling of ores, with and without additives, to facilitate the comminution process (the reduction of particle size) is not new. The early potential of ball milling for the reduction and extraction of ores, however, has generally not been fulfilled, and interest in such ore processing technology has waned. The development of a new form of high energy ball mill at The Australian National University, and the success that has been achieved in mechanical alloying work with that ball mill (see, for example, the

- 5 -

specifications of International Patent Application Nos. PCT/AU91/00248, PCT/AU92/00073 and PCT/AU94/00057, have stimulated new interest in the cold milling of ores. That new ball mill, which is described in the specification of International Patent Application No. PCT/AU90/00471 (WIPO Publication No.

5   WO91/04810), enables controlled energy milling of a charge to be effected. The present inventors have now discovered that under certain milling conditions, minerals containing silica, such as zircon, can be reduced while being converted into a nanostructural form, and that silica and other minerals can be removed from this product (for example, using hydrochloric acid).

10

Summary of the Invention

In it's broadest form, the present invention provides methods for production of a magnetic powder using ball milling.

15   In a first aspect, the present invention provides a method of production of a desirable magnetic powder from reduction of an oxide, comprising the steps of:

providing a mixture of oxide and a reducing agent (dispersing liquid);

controlled milling said mixture in a substantially low oxygen pressure environment to effect transformation of said oxide to a magnetic powder.

20

Preferably, said oxide comprises hematite (Fe_2O_3), and wherein said magnetic powder comprises magnetite (Fe_3O_4).

Preferably, in said controlled milling step, substantially complete transformation

25   of hermatite to magnetite is effected.

Also preferably, said reducing agent comprises water.

Also preferably, said environment is substantially oxygen-free.

30

Also preferably, said milling step is performed as low-energy milling.

In a second aspect, the present invention provides a method of production of

- 6 -

magnetic power , comprising the steps of:

milling a complex magnetic oxide. using a high energy milling device; and.

annealing said milled product at a temperature of above about 700K (i.e.

combined mechanical and chemical activation).

5

Preferably, said annealing step is performed at about 1200K to 1600K for about

1-6 hours.

Perhaps most preferably, said annealing step is performed at about 1273K.

10

In a preferred form, said milling step is performed in dry conditions in a vacuum,

air or other gas atmosphere.

Preferably, depending on pressure and gas atmosphere, particle size and size

15   distribution of said milled product can be influenced.

Also preferably, said particle size of said milled product is about 0.1 to 0.5 μm,

when milled in air, or about 1 μm when milled in a vacuum.

20   In another preferred form, said milling step is performed utilising an organic

solvent.

In a preferred embodiment said magnetic oxide is barium ferrite ($BaFe_{12}O_{19}$).

25   Preferably, said milling for both methods is effected in a ball mill of the type

described and claimed in the specification of International Patent Application No.

PCT/AU90/00471.

Brief Description of the Drawings

30   The present invention will become more fully understood from the following

description of a preferred but non-limiting embodiment thereof, described in connection

with the accompanying drawings, wherein:

- 7 -

Fig. i illustrates a schematic diagram of the various iron oxides phases:

Fig. 2 illustrates the temperature versus oxygen pressure (T-PO$_2$) phase diagram of the iron-oxide system;

Fig. 3 shows a SEM microphotograph of a barium ferrite (BaFe$_{12}$O$_{19}$) powder used in the experimental procedure herein described;

Fig. 4 illustrates XRD evolution patterns of barium ferrite powder milled in air for different periods of time;

Fig. 5 illustrates XRD evolution patterns of barium ferrite powder milled in vacuum for different periods of time;

Fig. 6 shows the results of SEM analysis of powder morphology versus milling time performed on air (a) and vacuum (b) milled samples;

Fig. 7 shows the results of SEM analysis of V1000 powder particles;

Fig. 8 shows a TGA scan for as milled powders a) A1000 and b) V1000;

Fig. 9 illustrates the fragmentation (a, b and d), consolidation (e) and decomposition mechanism (c) occurring during prolonged ball milling of barium ferrite in air (a-d) and vacuum (a-b-e);

Fig. 10 illustrates magnetic hysteresis curves of unmilled barium ferrite (BaFe$_{12}$O$_{19}$) and some milled powders from Table I annealed at 1273K;

Fig. 11 illustrates a schematic diagram of a suitable mill used during method of the present invention;

Fig. 12 shows x-ray diffraction (XRD) patterns of hematite milled in wet conditions (water): and,

- 8 -

Fig. 13 illustrates the intensity ratios between XRD reflexes from (104) and (110) planes of the hematite structure versus milling time.

5   **Detailed Description of Preferred Embodiment(s)**

A preferred but non-limiting embodiment of the invention will be hereinafter described in relation to an actual experimental procedure, describing the results and conclusions drawn therefrom. It should be noted that this embodiment is provided for the purpose of understanding the invention, but, the invention should not be considered
10   to be limited to the described embodiment.

METHOD 1

EXPERIMENTAL PROCEDURE

Material

15   As starting material commercially available pure (99.99% wt.) barium dodecairon nonadecoxide $BaFe_{12}O_{19}$ ferrite powder with particle size distribution in the 0.5-50 μm range (from Alfa Products/Jonhson Matthey) was used. Powder examination by X-ray diffraction (XRD) technique shows perfect hexagonal structure with space group P63/mmc. This is characteristic of M-type ferrites. Fig. 3 shows micrographs from
20   scanning electron microscopy. In Figs. 4 and 5 the XRD pattern of pre milled powder is included, to be compared with milled material.

Experimental procedure

Prior to milling two powder samples (each 10 g in weight) were annealed for 1
25   hour at -700 K to remove adsorbed water molecules. The milling in air and "normal" vacuum (10^{-1} - 10^{-2} Pa) was conducted in a vertical stainless steel mill (Uni-Ball) operating in high energy mode. Four 67 g magnetic steel balls with chrome hardened surfaces were employed for milling. The effective mass of ball in the external magnetic field used during milling was -600 g and ball to powder weight ratio was ~60:1. The gas
30   atmosphere inside the vial was controlled by a pressure valve. In this way both air under normal pressure, and a vacuum, were employed in the preparations. Samples were taken from the vial at different stages of milling (190 h, 360 h, 590 h, 690 h and 1000 h) for morphological and structure analysis. Particle morphology was examined by direct

- 9 -

observation of gold coated samples on a Jeol SEM 6400 scanning electron microscope The structural characterisation was performed using a Philips X-ray powder diffractometer employing $CoK\alpha$ (λ = 1.789 am) radiation (scan rate 2 deg/min with CD-ROM JCPOS-database and PC fitting program for detailed analysis of XRD patterns.

5   Thermogravimetric experiments were performed in a Shimadzu TGA-50H thermoanalysis system, on -20 mg of material under dynamic pure argon atmosphere with flow rate 50 ml/min. The temperature sweep rate was 30 deg/min for TGA.

RESULTS AND DISCUSSION

10   *XRD of Ba-ferrite powder milled in air*

The X-ray diffraction patterns of the materials obtained on milling $BaFe_{12}O_{19}$ powder in air for different periods of time are shown in Fig. 4. As can readily be seen several distinctive features occur on ball-milling in comparison with the XRD pattern for the pre-milled powder.

15

Firstly, commensurate with significant peak broadening, the intensities of all of the diffraction peaks decrease with milling time. Indeed, for a sample milled for 190 hours the peaks are about twice the widths of the peaks in the starting material. A second development is the broad feature in scattering which extends over the very wide

20   angular range $2\theta = 25° - 50°$. The extent of this broad peak, centred at $2\theta = 37.0° \pm 0.1°$ (190 h); $37.5° \pm 0.1°$ (360 h); $36.8° \pm 0.2°$ (590 h); $38.6° \pm 0.4°$ (690 h) and $38.7° \pm 0.3°$ (1000 h) was further characterised for different milling times using a standard XRD fitting program with a capacity to analyse a maximum of 15 peaks at the same time. The discernible peaks in the $2\theta = 25° - 80°$ range were fitted individually, allowing the broad

25   feature to be described by a Gaussian curve of full width at half height $\Delta(2\theta) = 9.8° \pm 0.2°$ (190 h); $12.1° \pm 0.3°$ (360 h) and $12.4° \pm 0.5°$ (590 h, 690 h and 1000 h). This broad peak is located near the position of the most intense reflection from the (107) plane of the Ba-ferrite crystal structure ($2\theta_{107}$ - 37.51°). From the analysis of the fits to the XRD data over the scattering region 25°-55°, the following values for the fractional

30   area of this broad feature, A_b, as a function of the milling times were found; A_b = 65% (190 h); = 72% (360 h); = 81% (590 h); = 68% (690 h) and = 45% (1000 h). This behaviour, with a maximum in the intensity of the broad peak after 590 hours of milling is evident from the overall trend of the XRD patterns shown by Fig. 4 The intensities

- 10 -

of all the peaks decrease with milling time (190 - 360 h), with a tendency for new peaks to occur for longer milling time (690 - 1000 h). The XRD pattern of the sample milled for 1000 hours allows a semi quantitative analysis of the discernible peaks. In particular the (107)- 37.5°, (114)- 39.8°, (205)- 47.16°and (206)- 49.7° reflections of hexagonal Ba

5   ferrite can be indexed along with the following dominant lines of the hematite α-Fe_2O_3 structure (012) - 28.1°, (104) - 38.7°, (110) - 41.6°, (113) - 47.8°, (024) - 58.2° and (116) - 63.7°. The partial decomposition of $BaFe_{12}O_{19}$ phase to α-Fe_2O_3 and BaO on ball-milling in air is not unlikely, assuming the compositional make-up of barium ferrite ($BaO.6Fe_2O_3$) and the α-Fe_2O_3 stable at room temperature structure (resistant to extended

10   dry or wet milling in air [5]).

Indeed, the most intense Ba-ferrite XRD reflection $2\theta_{107}$ - 37.510° transforms into the strongest line for hematite $2\theta_{104}$ = 38.694°. During continuous mechanical activation the starting powder undergoes transformations, the most obvious of which are colour

15   changes of the powder. The 1000 hours ball-milled sample A1000 is dark reddish-brown, remarkably different from the dark brown pre-milled $BaFe_{12}O_{19}$ powder. For each milling period particular colour change is a consequence of specific structure transformations shown in Fig. 4.

20   *XRD of Ba-ferrite powder milled in vacuum*

Fig. 5 shows the XRD pattern evolution for $BaFe_{12}O_{19}$ powder processed in vacuum. The decrease of the peak intensities and continuous broadening of the Bragg peaks are evidence for the formation of a nanocrystalline phase and the effect is similar to that described above for air milled powder. The most evident changes here in

25   comparison with Fig. 4 are the absence of strong material decomposition for the 690 h and 1000 h milled powders. However, for the V1000 sample a weak tendency for the onset of new peaks can be observed. By employing the same XRD fitting program with a Gaussian shape to data from Fig. 5 it was found that the broad feature for which milling time is centred and has fill width at half height; 2θ = 38.2° $\pm$ 0.7° and $\Delta 2\theta$ =

30   13.7° $\pm$ 0.4° (190 h); 37.5° $\pm$ 0.5° and 13.9° $\pm$ 0.4° (360 h); 36.8 $\pm$ 0.5 and 10.3° $\pm$ 0.3° (590 h); 36.6° $\pm$ 0.2° and 11.1 $\pm$ 0.4° (690 h); 36.4° $\pm$ 0.3 and 10.4° $\pm$ 0.5° (1000 h). It is clear from the above that the $2\theta_{107}$ peak position is shifted to lower values with increasing milling time. Thus, the d_{107} spacing of the Ba-ferrite structure increases for

- 11 -

vacuum milled powder contrary to the trend observed for air milled powder. We attribute this effect to mechanically induced structural deformations (responsible for long range disorder) of vacuum ball-milled material. For air milled powder the structural decomposition of Ba-ferrite is due to high oxygen gas adsorption on the particle

5   surfaces. This effect will be clarified from detailed analysis of thermo-gravimetric data described below. From an analysis similar to that above of the fits to the XRD data over the scattering region $25° - 55°$, the following values for the fractional area of the broad feature, A_b, as a function of the milling times were found $A_b = 65\%$ (190 h); $= 76\%$ (360 h); $= 78\%$ (590 h); $= 80\%$ (190 h) and 79% (1000 h). These values agree well with

10   the behaviour described qualitatively above. We conclude that in powder milled in vacuum the disordering process is continuous. As was mentioned above, for the 1000 hours milled sample V1000 a weak tendency for reordering has to be taken into consideration. In this way, the observed structural changes are different for air and vacuum milled powders. In Figs. 4 and 5 the XRD patterns show similar results for

15   A1000 and V1000 samples, where the crystal structure of premilled Baa-ferrite is perfectly restored. Additionally, it is found that annealing in air or vacuum has no influence on the final powder structure.

SEM analysis of Ba-ferrite powder milled in air

20   SEM micrographs of pre-milled material are given in Fig. 3. A broad dispersion of particle size is visible, although most are in the range 1 - 10 μm. The shape of the particles can be best characterised as highly irregular. In Fig. 6 (a) results of SEM analysis performed on air milled Ba-ferrite powder are presented (samples A190-A1000). On each photograph the milling times is shown in the top left corner. The particle

25   morphology is very different from that of the starting material. Independently of milling time all particles have a more spherical shape with particle size decreasing with increasing milling time. The final 1000 hours milled sample shows the smallest particles, with average size 0.3 μm. As the milling progresses, the powder was found to be more homogeneous. Particles above 1 μm can be found for powder milled up to 590 hours.

30   Longer time causes the powder to become homogeneous with particle size in the range 0.1 - 0.5 μm (A1000).

SEM analysis of Ba-ferrite powder milled in vacuum

In Fig. 6(b), SEM micrographs of Ba-ferrite milled in vacuum are presented. It was found that grinding in a vacuum yields a different particle morphology compared to samples processed in the same time period in air. There is not such an apparent particle size decrease with milling time as in air. After the first 590 hours the size

5   remains essentially constant. The average particle size is close to 1 μm even after 1000 hours. Similar reshaping (to spherical) and initially characteristic stepped surfaces can be observed, but for the last sample V1000, a different surface morphology is visible. This effect is milling time dependent and Fig. 7 shows typical details in higher magnification. In micrograph (a) the cluster of small -1 μm particles around a larger

10 one ~10 μm is visible. We assume that the effect is due to strong magnetic interactions where the largest particle has a higher magnetic remanence. This will be discussed in detail below. In the course of milling, the small particles and a large one are "alloyed" together. This behaviour is similar to mechanical alloying of metal particles where simultaneous plastic deformation and fracture of powder particles coexists. In the next

15 stage the particle surface evolves. It was found to be irregular, but the whole particle remains spherical. The surface layer seems to be highly disordered with crystal grains below 50 nm and the amount of these particles increases with milling time. On this point, it is easy to understand why, for Ba-ferrite powder, the particle size remains above - 1 μm. The operating mechanism is similar to mechanical alloying. rather than a

20 simple fracturing process as occurs for the air milled sample. The nature of this behaviour will be addressed below.

Thermogravimetric Analysis

In Figs. 8(a) and 8(b) the results of thermo-gravimetric analysis (TGA) of A1000

25 and V1000 powders show directly the composition difference between each type of as milled sample. The observed weight decrease for air milled powder in the temperature range of 330-1070 K has a significantly high value of 6.62 wt. %. It was identified that oxygen loss (desorption) is mainly responsible. The final weight decrease in the temperature range of 920-1070 K can be attributed to barium ferrite structural

30 restoration. The number of oxygen molecules O_2 per one crystallographic Ba-ferrite unit cell (2 x $BaFe_{12}O_{19}$) at room temperature can be obtained by calculation from the weight loss and was found to be ~1.2. This result shows that, on average, nearly one additional oxygen atom is connected to one Ba-ferrite molecule, forming either a surface layer or

- 13 -

diffusing inward through grain boundaries or micro cracks. At the present time it is difficult to discuss this "superoxide formation" situation in detail because of the unknown nature of bonding. A TGA scar for vacuum milled material in Fig. 8(b) shows a different thermal characteristic of weight loss factor, with 10 times lower magnitude.

5   Weight loss can be observed in a narrow range of temperature 570-820 K. Subsequently weight increases over a much broader temperature range, 820-1270 K. We assume that trace gas desorption occurs up to 820 K as the nanocrystalline structure is under thermal stress relaxation, and then barium ferrite crystal grain growth requires oxygen (argon used in TGA experiments has minimal O_2 contamination) to fill up its vacancies. The

10   same effect is visible for sample A1000 in the high temperature range (cf. Fig. 8(a)). During thermal treatment (4 h at 1273 K) of both powders, a regrowth of grains of the ordered phase occurs. For the V1000 sample it can be more accurately described as a transformation process between nanostructured or disordered material and an ordered crystalline phase.

15

Magnetic properties

From early reports on magnetic properties of milled barium ferrite, is has been well established that magnetic properties are greatly affected by milling and annealing processes. The inventor's findings confirm these conclusions. From the results of

20   hysteresis measurements performed at room temperature presented in Table I and Fig. 10, it is clear that for as-milled samples A1000 and V1000 all parameters are extremely low by comparison with the premilled powder $BaFe_{12}O_{19}$. After subsequent annealing 4 hours at 773 K only minimal changes of hysteresis parameters are observed. The most significant improvement of overall magnetic properties was recorded for powders

25   annealed 4 hours at 1273 K. Magnetic hysteresis curves for some of these powders are presented in Fig. 8, for the parameters listed in Table 1. Furthermore, we note that after annealing at 1273 K hysteresis parameters (see Table I and Fig. 10) are weakly dependent on the air pressure during milling. However, slightly higher M_s values were observed for air milled powders AA1273 and AV1273. On the other hand annealing in

30   air promotes minimally higher H_c values. We assume that different particle morphology, as seen in Fig 6, is directly responsible for magnetic parameter value fluctuations. It is obvious that, independent of particle size for either air or vacuum milled powders, the observed M_s values are close to values measured for a starting powder (-90%), but of

importance is the fact that the coercivity increases over six times and reaches a value 445.6 kA/m. Because the final particle size of annealed A1000 and V1000 powders is significantly different, similar H_c values recorded for these samples is attributable to the same crystal grain size due to the identical thermal treatment. Such high H_C values are typical of chemically coprecipitated fine Ba-ferrite powders, where perfect crystal structure assures a defect and stress-free spin arrangement with high magnetocrystalline anisotropy. According to the Stoner and Wohlfarth theory of coherent rotation, the theoretical coercivity for a random assembly of Ba-ferrite particles would be $H_c = 0.96$ $K_1/M_s = 664$ kA/m (substituting $K_1=+33$ MJ/m^3 and $M_s=390$ kA/m). This theoretical value is higher than any value ever obtained on mechanically processed and annealed powders.

TABLE 1

Values of magnetic hysteresis parameters: M_s - volume saturation, M_r - remanence and H_c - coercivity. All parameters measured at room temperature. Maximum magnetic field applied I T. Second letter in sample description: A - annealed in air and V - annealed in vacuum.

Sample	M_s (kA/m)	M_r (kA/m)	H_c (kA/m)
$BaFe_{12}O_{19}$	380.0	254.7	74.4
A1000	13.0	2.7	44.6
AA773	28.4	5.3	99.5
AV773	52.1	25.2	187.8
AA1273	347.8	222.8	445.6
AV1273	344.1	203.5	393.9
V1000	13.8	3.2	35.0
VA773	13.0	3.6	58.5
VV773	22.9	5.6	60.9
VA1273	335.4	197.6	434.5
VV1273	343.0	199.2	429.7

- 15 -

Gas influence on fragmentation and consolidation

The above discussion is concerned predominantly with the distinguishing differences between structural, thermal and magnetic properties of powders milled in air and vacuum. The milling process is now characterised more carefully. The influence of gas pressure during milling on material morphology and structure is highlighted. In the case of prolonged ball milling of barium ferrite it is found that air pressure is an important factor determining the final particle structure and morphology. Results of milling in air show good agreement with previous findings, where milling time dependent chemical decomposition was observed. However, up to this time the mechanism of this process remains unaddressed. It is noted that decomposition of complex oxides into simple oxides is directly connected with the presence of air during milling. Furthermore, on the basis of normally expected high reactivity of oxygen compared with other gas elements in air, it is assumed that presence of O_2 molecules mostly influences milled material even if it is already an oxide. The influence of other gases, in our opinion promote only separation between powder particles by surface layer adsorption. Only oxygen is an active reactant at the oxygen-oxide interface, and, in Fig. 9 a suggested mechanism is presented schematically. It is obvious that a short milling time (up to 360 h) produces only particle size reduction by typical fragmentation and size homogenisation processes. Final powder particles have submicron size with a narrow distribution (cf. Fig. 6). By application of further milling, effects of oxygen oxide interface are more effective due to surface Fe-O bond rupture. The last effect involves electron transfer within anionic and cationic sublattices. With influence of metal surface (mill and balls), in the oxygen-oxide interface existing electric field gradient can be effectively cancelled by chemical potential difference. Gradients of cations Fe+ and anions 0- tend to give charge transport leading to the reverse electrical polarity. Existence of opposite ionic currents J (ci, ai - cation and anion interstitials, cv, av - cation and anion vacancies) generate diffusion and, finally, complex oxide decomposition can take place as a result of different diffusion rates for iron and barium (cf. Fig. 9 c-d). Furthermore, a nonmagnetic Fe_2O_3 surface layer promote separation of small particles during milling in magnetic field. Contrary to this vacuum milled powder behaves in a different way. Continuous mechanical activation results in a consolidation process and formation of structurally disordered ferrite particles (cf. Fig. 7 and 9 e). Finally, by

- 16 -

using relatively short annealing time at 1273 K short range diffusion is sufficient for nucleation of nanocrystals of Ba-ferrite in air as well vacuum milled material. with extremely high magnetic coercive field. Further experiments are being undertaken to find information concerning changes in microstructure related to improvement of magnetic
5   properties.

METHOD 2
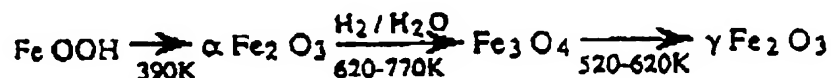
EXPERIMENTAL PROCEDURE

        The experimental details of first, complete transformation of hematite into high
10   purity magnetite (no other phases or contamination can be detected) as reported. Results of ball milling experiments performed in different conditions are analysed to obtain phenomenological characterisation of the process. The milling for all samples (8g in weight) was conducted in vertical stainless steel mill (Uni-Ballmill) operating in low energy mode. The ball-to-powder weight ratio was -30:1, Fig. 11 shows a schematic
15   diagram of the mill used in the experiments.

        We have to stress that an important aspect of this device is the application of a magnetic field generated by permanent magnet(s) to ferromagnetic balls. Depending on the distance between balls and magnet the effective mass of the ball can be increased
20   by a factor of -80 (from 650 g up to 5 kg), and by changes of the magnet(s) position, the type of energy transferred to the milled material can be varied. Thus, for magnet positions (1-3) indicated in Fig. 11, it is found that for M1 the energy is frictional type. M2 is mainly kinetic and for M3 both types are realised. In this way the high energy mode can be arranged by choosing magnet positions M1, M2 or M1+M2. For the low
25   energy mode which was used in the present experiment, the magnet was in position M3 with a "mass factor" of -80.

        The hematite (α-Fe_2O_3) analytical purity 99.9% powder with particle size distribution into range 20-70 µm (from Koch-Light Labs. Ltd., England), was introduced
30   into the vial with or without dispersing liquid (5 ml) and sealed. The gas atmosphere inside the vial was controlled by a pressure valve. In this way air, argon, and low or high vacuum were used in the preparations.

- 17 -

RESULTS AND DISCUSSIONS

Fig. 12 shows the time evolution of XRD patterns of milled hematite in wet conditions. In this experiment before the milling started, the air was removed and consequently after each vial opening to take samples. As can be seen, after 70 hours of

5   milling the hematite - magnetite transformation was complete. The product was found to be pure magnetite with perfect cubic crystallographic structure, described by space group Fd3m. Particle size distribution was decreased from 70-20 μm for α-Fe_2O_3 to the micron range of 2-0.1μm for the final product. No other phases or amorphization effects were observed during processing or thereafter. No significant contamination

10   from mill was detected (the mass of the balls remain constant). Thus, this situation the most possible reduction reaction mechanism that comes to mind to account for the phenomenon, namely $4Fe_2O_3 + Fe \Rightarrow 3Fe_3O_4$, can not be considered. The same situation holds if we consider another typical reaction for reduction of iron oxides. Normally the chemical reduction steps of the transformation of FeOOH into γ-Fe_2O_3 through the well

15   known process

$$Fe\,OOH \xrightarrow[390K]{} \alpha\,Fe_2\,O_3 \xrightarrow[620\text{-}770K]{H_2/H_2O} Fe_3\,O_4 \xrightarrow[520\text{-}620K]{} \gamma\,Fe_2\,O_3$$

20   have to be carried out at a temperature low enough to prevent particles sticking, or recrystallisation into bigger crystalline grains, but high enough to produce the required modification. This conventional "high temperature approach" to hematite - magnetite transformation is not relevant to the process presented here. The present process occurs at low temperature, without any typical reducing agent like hydrogen or carbon.

25

Effects of the transformation are clearly visible if the intensity ratio between XRD reflection from (104) and (110) planes of the hematite structure are compared. This type of graphical analysis of XRD patterns is possible because the (110) peak from hematite structure is near the (311) peak of magnetite. For a 1:1 mixture of hematite-

30   magnetite powders, the ratio between intensity of (104) and (110) + (311) peaks is equal to unity. In Fig. 13 experimental data for powders from Fig. 12 are included and marked with "vacuum" - small open square. Also, the other prepared powders are included. As can be seen, comparing with other processing conditions, wet milling in

- 18 -

low vacuum (-10^3 Pa) can be characterised as the fastest and total transformation of hematite into magnetite.

It is remarkable how rapidly and efficiently this process takes place. Indeed so surprising is the result that it raises many questions that require detailed answers. What are the main factors that determine this hematite - magnetite structural transformation? To answer this, other experiments were performed in parallel and the results are described below.

A.   Dry Milling

A range of conditions were taken. The milling in high vacuum with a pressure of 3-10^{-2} Pa was investigated. Prior to the milling, Fe_2O_3 and the mill were annealed at 800 K for 1 hour to remove all physically bonded water. After 170 hours of milling, the final pressure in the vial was higher, at 4 . 10^{-1} Pa and the resultant XRD pattern shows that only a weak reduction process occurs. It is concluded that it is not the high vacuum that is important. A "normal" vacuum (10^2-10^3 Pa), and particularly, wet milling conditions (water as in the first experiment), promote faster transformation (reduction). This can be partially understood in so far as wet milling induces faster particle size reduction than the dry process. Additionally, it was found that wet or dry processing has no influence on the reduction taking place, which suggest that a physical rather than chemical reduction mechanism is appropriate.

B.   Wet Milling

Some of the typical solvents used were: water, glycol (diethylene) and benzene compounds. The first two have dipolar molecules (polar type solvent) and the last one is a hydrocarbon.

The powder milled in benzene (air removed prior to milling) shows XRD pattern similar to that discussed above with dry powder milled in high vacuum. Addition of anthracene (benzene compound) as a reduction agent has the least effect on reduction process. Even after 200 hours of milling the crystallographic structure of the powder was unchanged. All other solvents (ionic) work better as can be seen from Fig. 13, and will be described below. All samples milled in ionic solvents can be divided into two

- 19 -

groups, with different air (oxygen) pressure during preparation. A sample milled in argon (4 . 10^5 Pa = 4atm) shows near full transformation after 100 hours. This indicates that oxygen partial pressure is the main influence on the milling time required for hematite reduction. Thus, it is not surprising that the slope of the "argon" curve in Fig.

5   13 is similar to the "vacuum" result.

By contrast, for α-Fe_2O_3 milled with water and under normal atmosphere pressure the reduction process is very slow. After 75 hours of milling , $I_{(104)}$ /$I_{(110)}$ = 1.20, and the intensity of XRD peaks are in the "noise" level. Thus, it is difficult to conclude that

10   reduction of hematite has occurred to any extent because there are probably other such effects, as XRD line intensity changes with decrease of powder particle size or shape. For the same powder after the first 75 hours of unsuccessful milling in air, further milling for 220 hours was conducted in the same mill with air evacuated from the vial. The filed small triangles in Fig. 13 show the subsequent observed XRD line intensity

15   behaviour. Full transformation occurs after - 220 hours and the process is 3 times slower than that for a sample milled directly without oxygen (vacuum or argon). It is noted again that the particle size influences the time required for transformation and the reduction mechanism is of physical rather than chemical origin. The effect of rupture of oxide surface layers under mechanical action may be taken into consideration, as well

20   as surface stress as a driving force for the reduction and removal of oxygen.

The last experiment in wet conditions was performed in diethylene glycol (boiling point b.p. = 518 K) as a dispersing liquid at temperature ~500 K (~20 degrees below the b.p.) to check the possibility of direct transformation of α-Fe_2O_3 into γ-Fe_2O_3.

25   The process assumed has to be either a two stage reduction: hematite- magnetite- maghemite, or direct hematite-maghemite. The results for the powders milled in air and vacuum show that even at elevated temperatures, only magnetite or phases mixed with hematite can be produced (cf Fig. 13).

30   Pure γ-Fe_2O_3 phase was obtained after application of annealing of "wet-vacuum" prepared magnetite in air at 500K. It is concluded that the last process has to be performed on dry Fe_3O_4 powder and direct transformation α- γ-Fe_2O_3 is not possible by mechanical activation.

- 20 -

In all the prepared samples described above, no other phases like Fe or FeO and any contamination were detected. Thus, low energy milling is most appropriate for hematite-magnetite transformations.

5   The experimental results presented here for method 2 clearly show that hematite-magnetite total transformation is possible by room temperature water assisted mechanical activation of α-Fe_2O_3 powder. It is suggested that oxygen bonds on the cleaved α-Fe_2O_3 oxide surface are broken during mechanical activation process and oxygen is released (removed) to the dispersing water or directly to vial internal space. It was found that

10   the oxygen pressure during the process as well the polar dispersing liquid or milling energy have a major influence on successful and fast phase transformation. All preparations performed in air, dry conditions or with hydrocarbons (benzene, anthracene) show that the process of hematite reduction is non existent, or at last very slow. Normal air pressure and/or use of hydrocarbons suppress the oxygen release. Contrary to high

15   energy milling performed by others we found that low energy milling is the most suitable for the transformation because the process has a physical rather than chemical origin.

It should be understood that the invention has been broadly hereinbefore

20   described with reference to particular embodiments and an actual experimental procedures Numerous variations and modifications will become understood to persons skilled in the art. All such variations and modifications should be considered to fall within the scope of the invention as hereinbefore described and as hereinafter claimed.

25

- 21 -

THE CLAIMS

1.   A method of production of a magnetic powder using ball milling.

2.   A method of production of magnetic powder, wherein said magnetic powder is
5   produced from an oxide, said method comprising the steps of:
         providing a mixture of oxide and a reducing agent (dispersing liquid);
         milling said mixture in a substantially low oxygen pressure environment to effect
transformation of said oxide to a magnetic powder.

10   3.   A method as claimed in claim 2, wherein said oxide comprises hematite (Fe_2O_3),
and wherein said magnetic powder comprises magnetite (Fe_3O_4).

4.   A method as claimed in claim 3, wherein substantially complete transformation
of hematite to magnetite is effected.
15

5.   A method as claimed in any one of claims 2 to 4, wherein said reducing agent
comprises water.

6.   A method as claimed in any one of claims 2 to 5, wherein said environment is
20   substantially oxygen-free.

7.   A method as claimed in any one of claims 1 to 6, wherein said milling step is
performed as low-energy milling.

25   8.   A method of production of a magnetic powder as claimed in any one of claims
1 to 7, comprising the steps of:
         milling a complex magnetic oxide, using a high energy milling device; and,
         annealing said milled product at a temperature of above about 700K.

30   9.   A method as claimed in claim 8, wherein said annealing step is performed at a
temperature of 1200K to 1600K for 1 to 6 hours.

10.   A method as claimed in claim 8, wherein said annealing step is performed at a

- 22 -

temperature of about 1273K.

11.   A method as claimed in any one of claims 8 to 10, wherein said milling step is performed in dry conditions in a vacuum, air or other gas atmosphere.

12.   A method as claimed in claim 11, wherein, depending on pressure and gas atmosphere, particle size and size distribution of said milled product can be influenced.

13.   A method as claimed in claim 12, wherein said particle size of said milled product is about 0.1 to 0.5 μm, when milled in air, or about 1 μm when milled in a vacuum.

14.   A method as claimed in any one of claims 8 to 13, wherein said milling step is performed utilising an organic solvent.

15.   A method as claimed in any one of claims 8 to 14, wherein said magnetic oxide is barium ferrite ($BaFe_{12}O_{19}$).

16.   A method as claimed in any one of claims 1 to 15, wherein said milling is effected in a ball mill of the type described in International Patent Application No. PCT/AU94/00471.

17.   A method of production of magnetic powder, substantially as herein described.

18.   A magnetic powder produced by the process substantially as herein described.

19.   A method of altering the magnetic coercivity of a product, substantially as herein described.

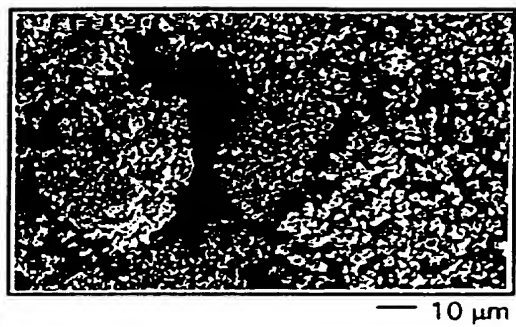20.   A product, having improved magnetic coercivity, substantially as herein described.
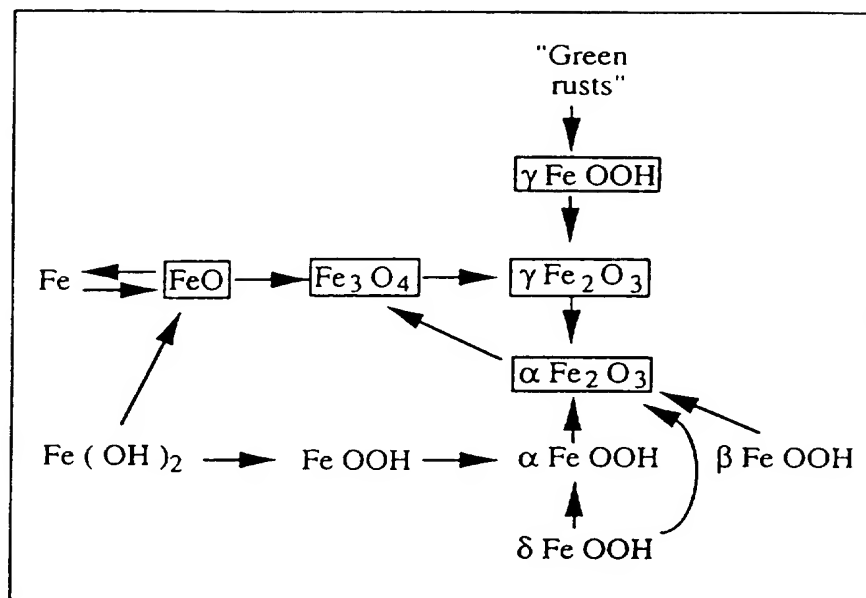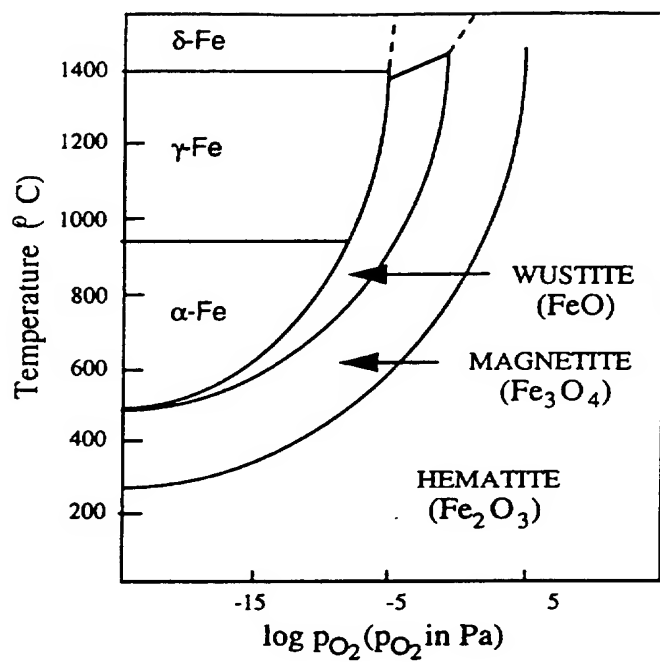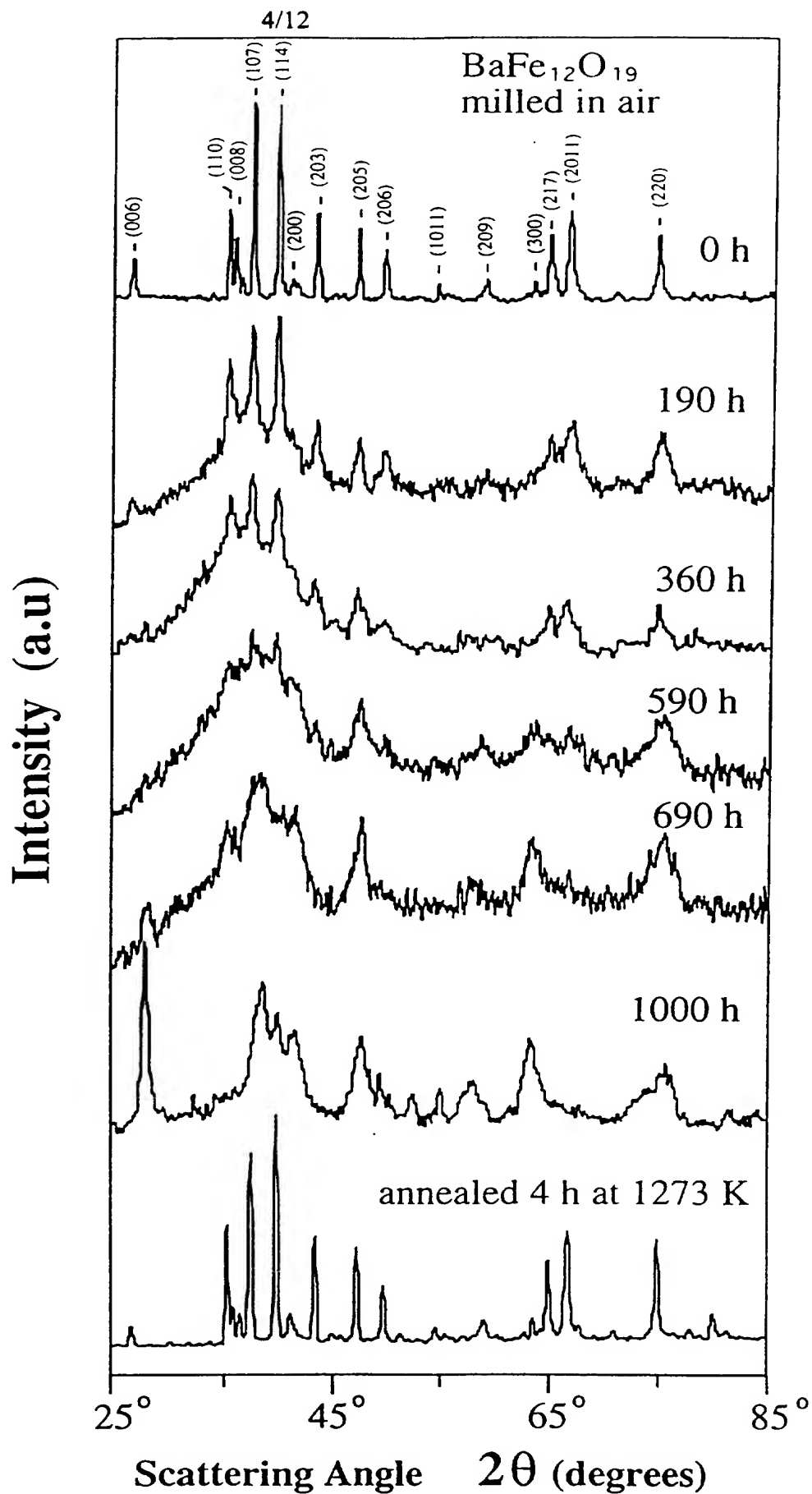
"Green rusts" → $\gamma\,FeOOH$ → $\gamma\,Fe_2O_3$

Fe ⇄ FeO → Fe_3O_4 → $\gamma\,Fe_2O_3$ → $\alpha\,Fe_2O_3$

$Fe(OH)_2$ → $FeOOH$ → $\alpha\,FeOOH$ $\beta\,FeOOH$

$\delta\,FeOOH$

FIGURE 1

FIGURE 2

— 10 µm

FIGURE 3

4/12

FIGURE 4
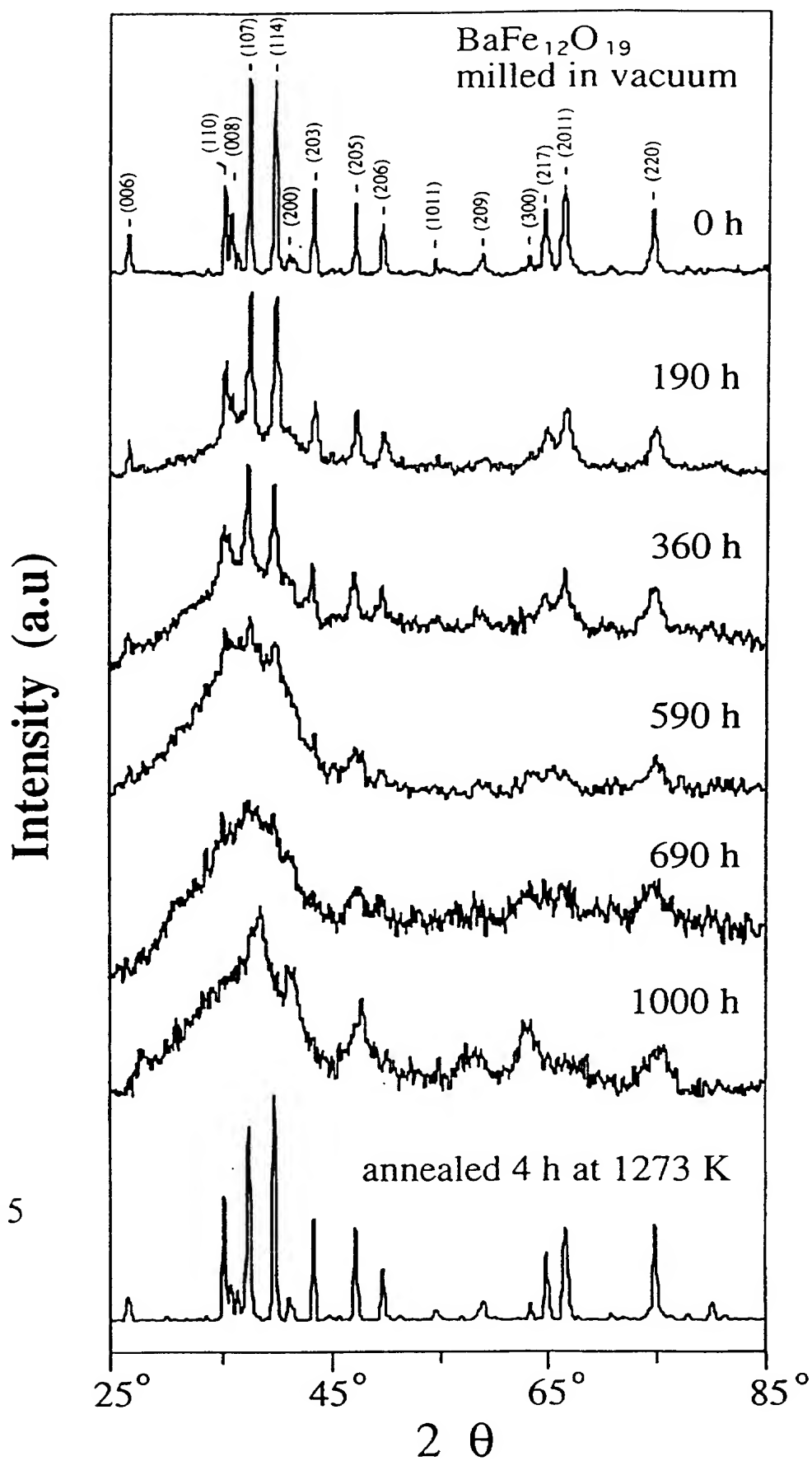
FIGURE 5

FIGURE 6

FIGURE 7

FIGURE 8

FIGURE 9

SUBSTITUTE SHEET (RULE 26)
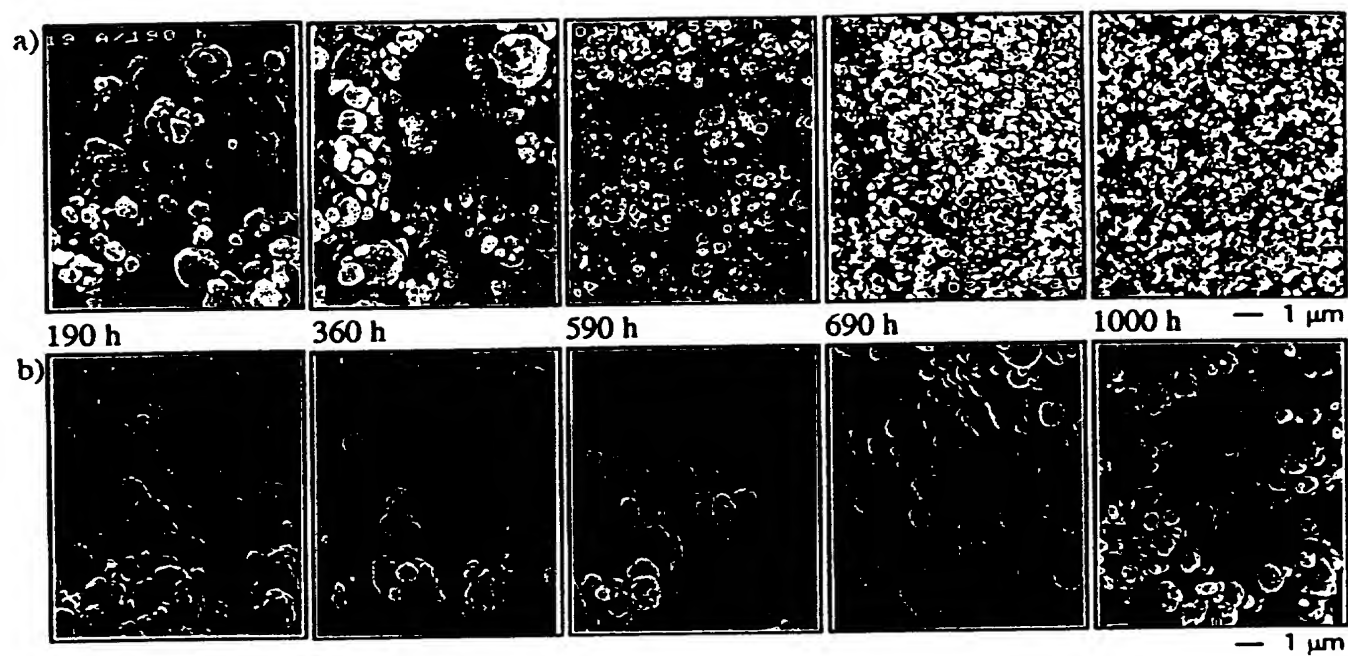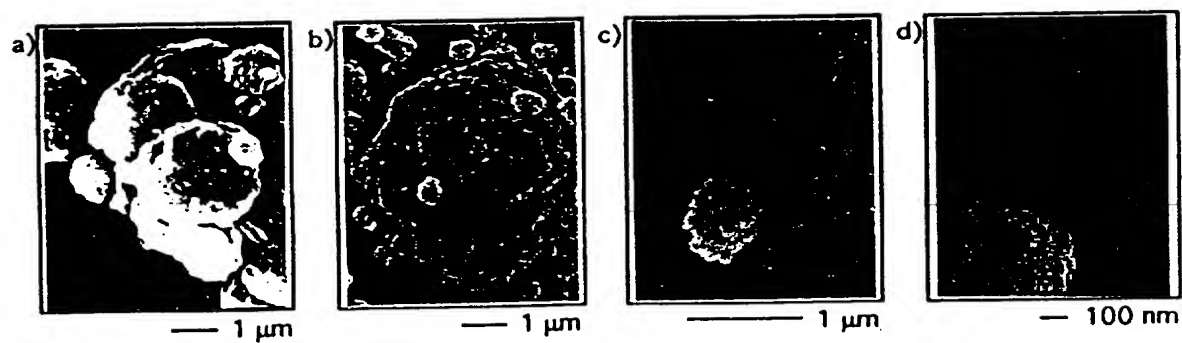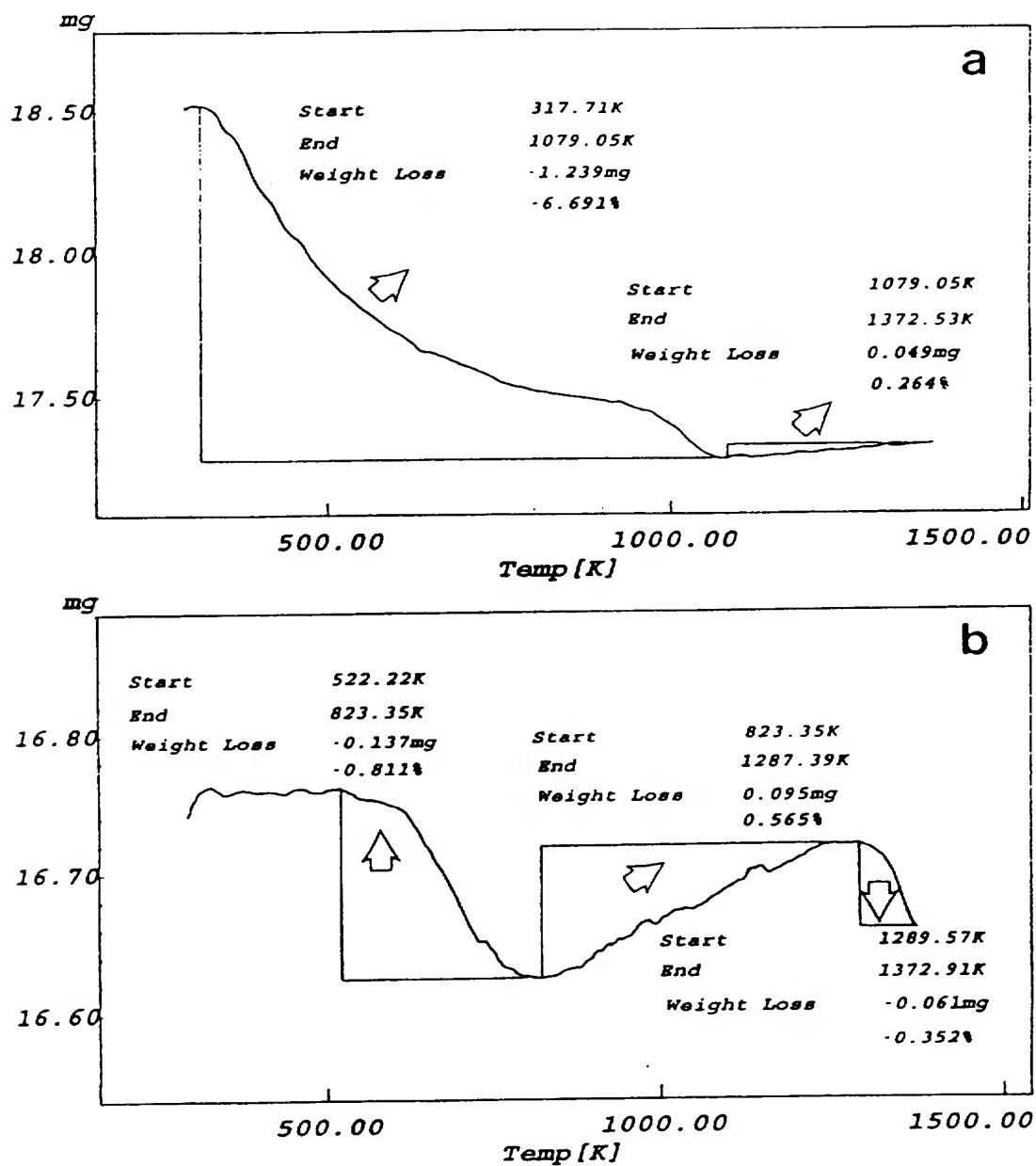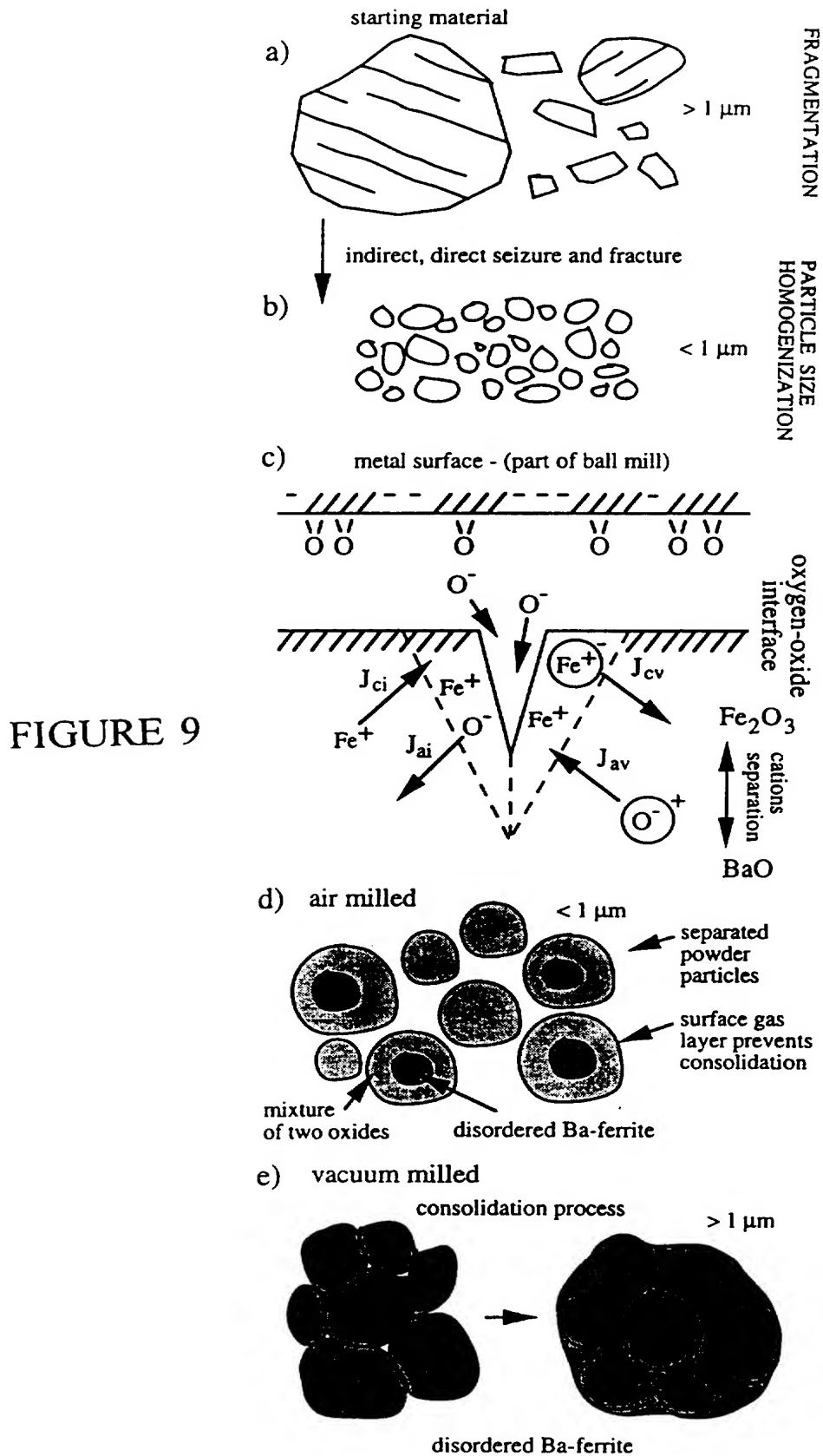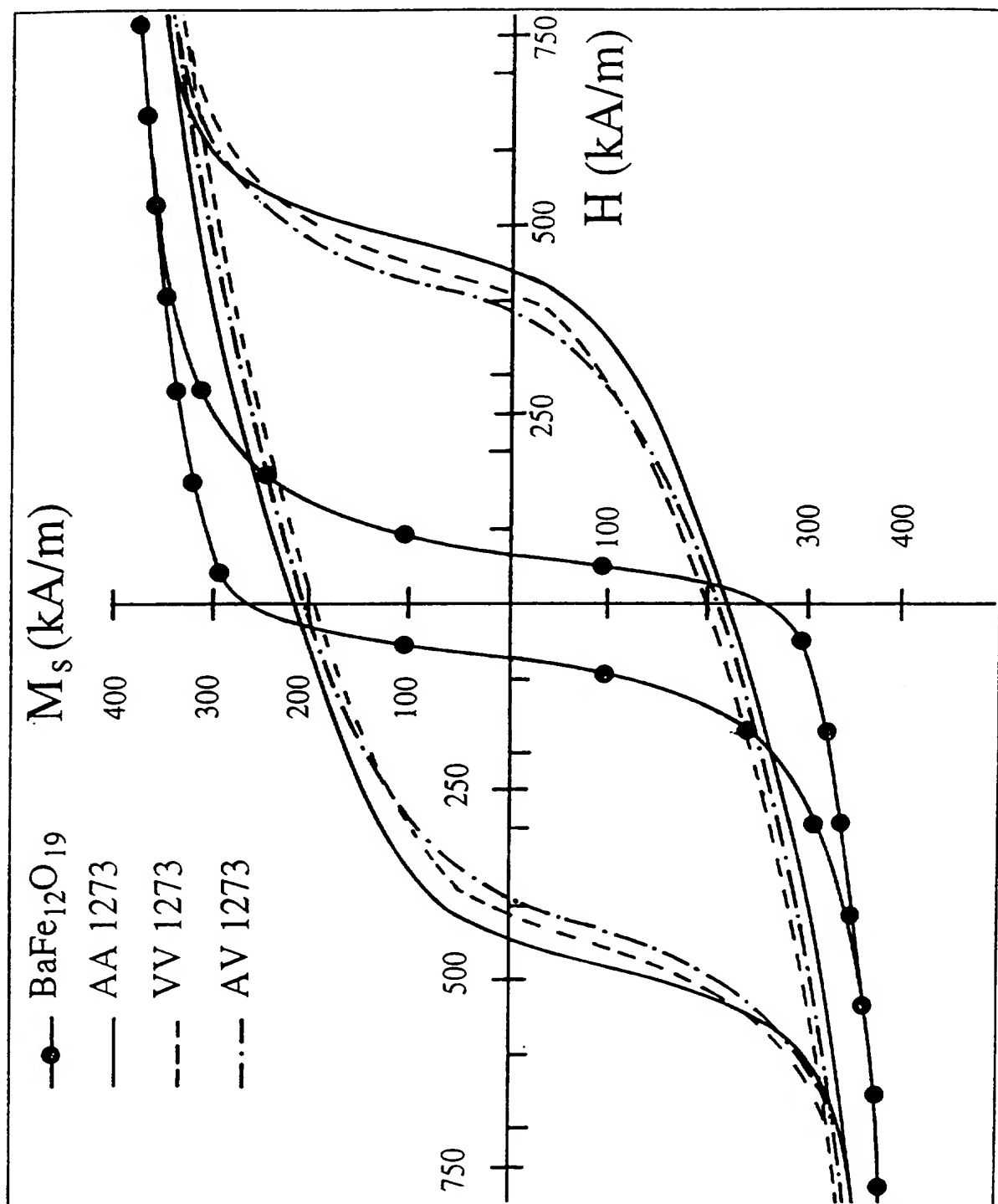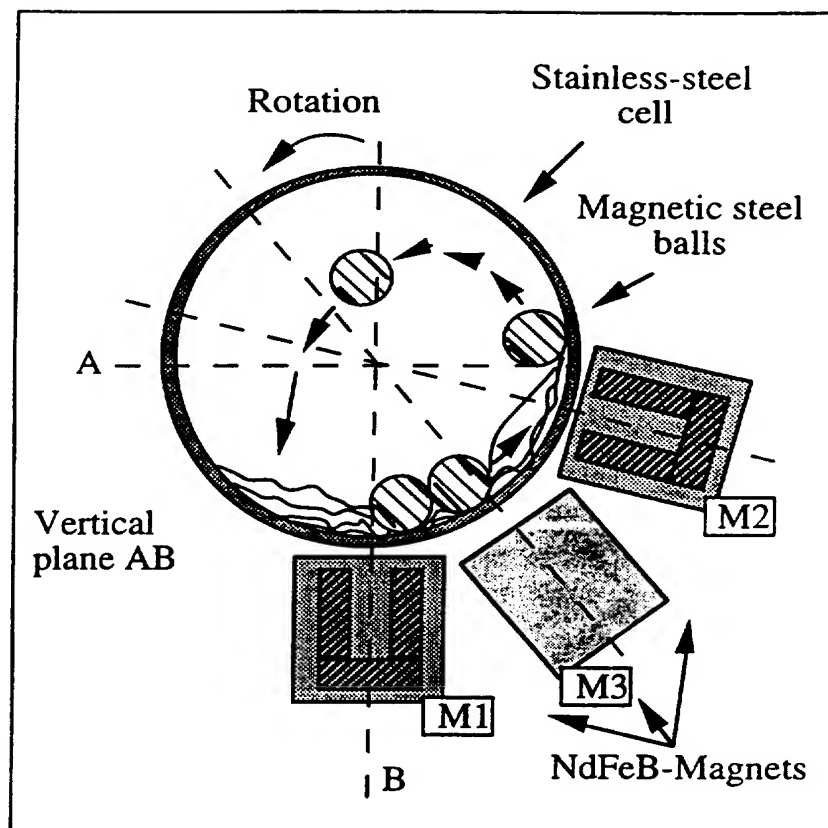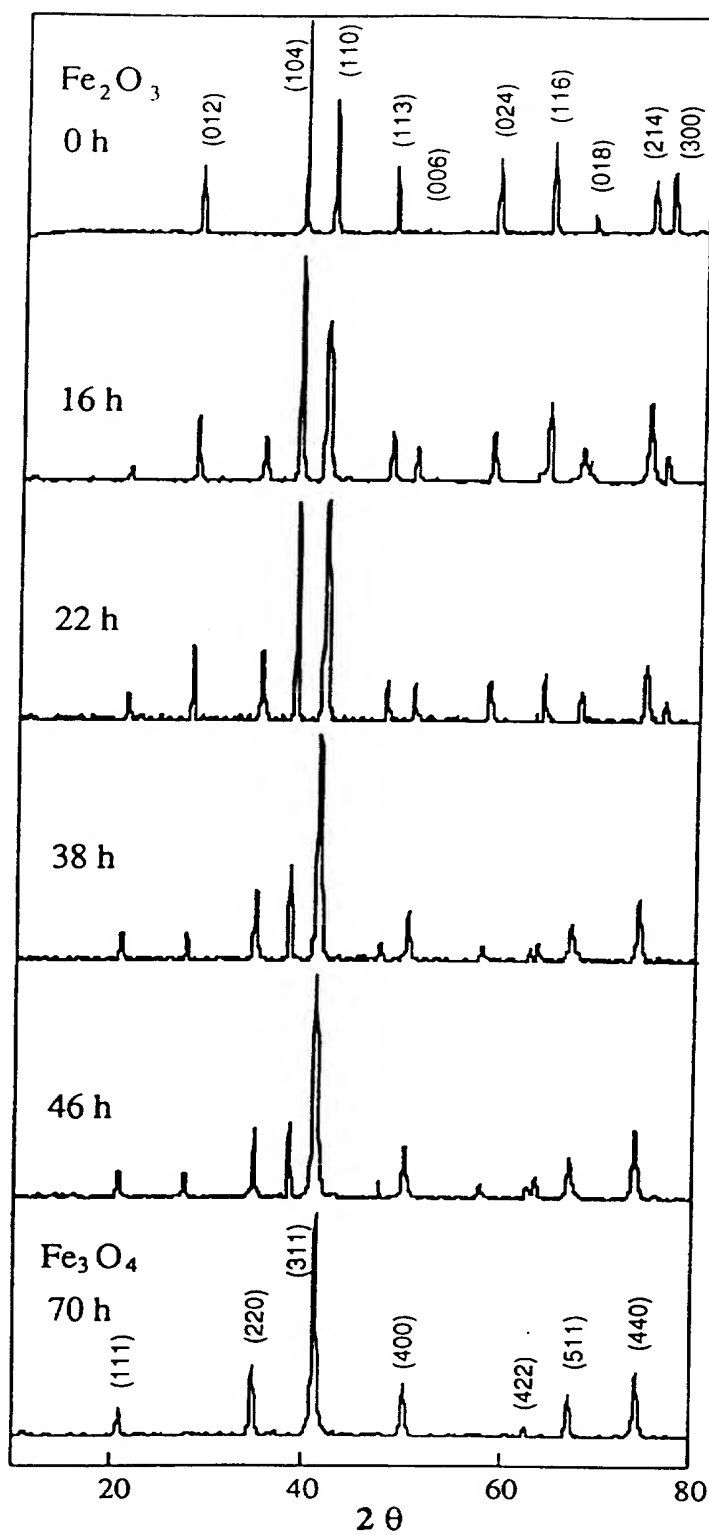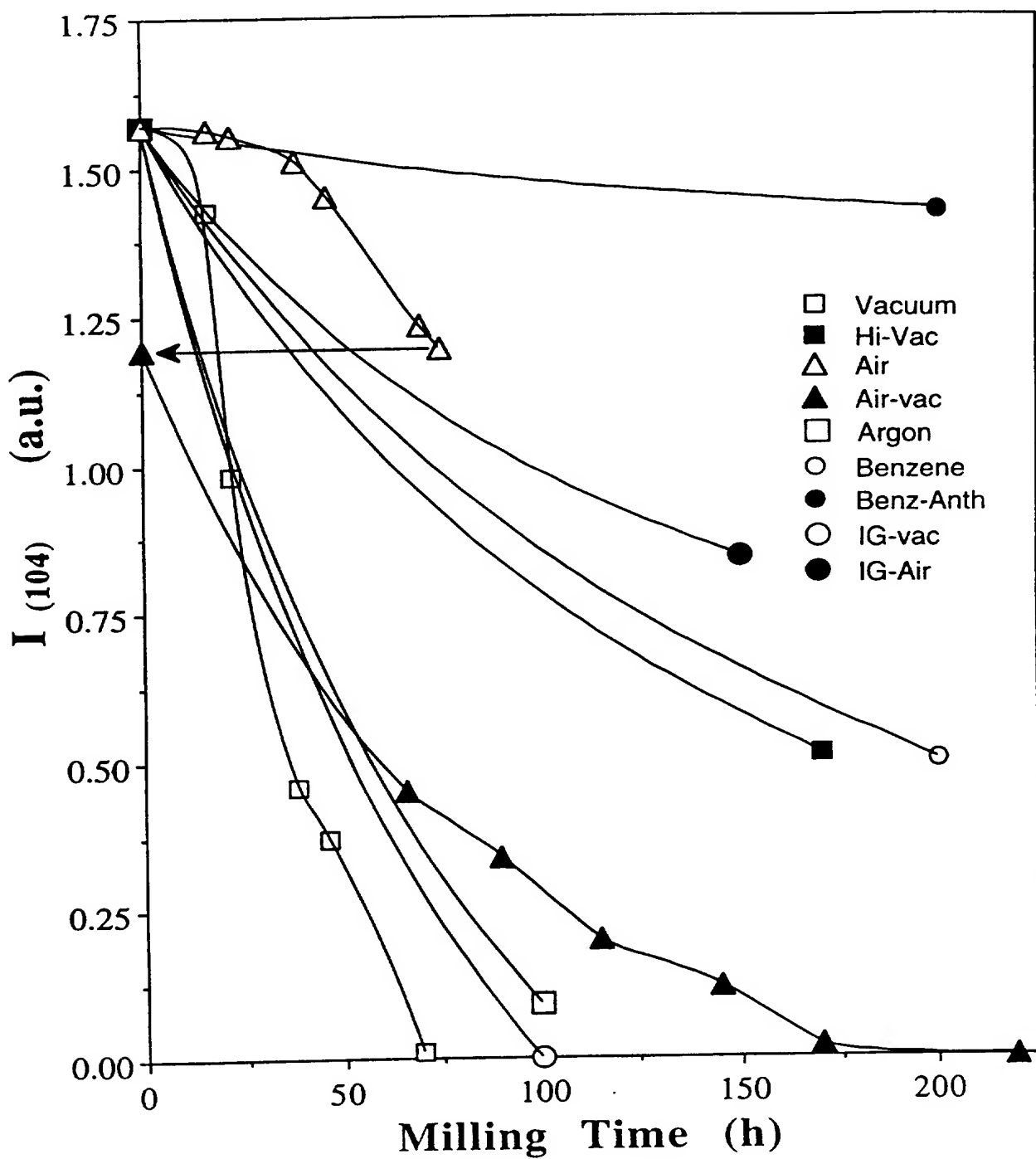
FIGURE 10

FIGURE 11

FIGURE 12

FIGURE 13

A.	CLASSIFICATION OF SUBJECT MATTER

Int Cl^6: C01G 49/08, B22F 009/04

According to International Patent Classification (IPC) or to both national classification and IPC

B.	FIELDS SEARCHED

Minimum documentation searched (classification system followed by classification symbols)
IPC C01G 49/48, B22F 009/04

Documentation searched other than minimum documentation to the extent that such documents are included in the fields searched
AU : IPC as above

Electronic data base consulted during the international search (name of data base and, where practicable, search terms used)
DERWENT

C.	DOCUMENTS CONSIDERED TO BE RELEVANT

Category*	Citation of document, with indication, where appropriate, of the relevant passages	Relevant to claim No.
X	DT 1 262 986 A (KNAPSACK AKTIENGESELLSCHAFT) 14 March 1968. See whole document.	1-12
X	Derwent Abstract Accession No. 91-244309, Class B06 E31 G01 L03, SU,A, 1611-870 (AS SIBE CATALYST IN (CSEK)) 7 December 1990.	1-7
X	EP 0 253 521 A (GENERAL MOTORS CORP.) 20 January 1988. See whole document.	1-8

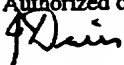| X	Further documents are listed in the continuation of Box C		See patent family annex

*	Special categories of cited documents:	"T"	later document published after the international filing date or priority date and not in conflict with the application but cited to understand the principle or theory underlying the invention
"A"	document defining the general state of the art which is not considered to be of particular relevance		
"E"	earlier document but published on or after the international filing date	"X"	document of particular relevance; the claimed invention cannot be considered novel or cannot be considered to involve an inventive step when the document is taken alone
"L"	document which may throw doubts on priority claim(s) or which is cited to establish the publication date of another citation or other special reason (as specified)	"Y"	document of particular relevance; the claimed invention cannot be considered to involve an inventive step when the document is combined with one or more other such documents, such combination being obvious to a person skilled in the art
"O"	document referring to an oral disclosure, use, exhibition or other means		
"P"	document published prior to the international filing date but later than the priority date claimed	"&"	document member of the same patent family

Date of the actual completion of the international search	Date of mailing of the international search report
19 December 1995	**08.01.96**

Name and mailing address of the ISA/AU AUSTRALIAN INDUSTRIAL PROPERTY ORGANISATION PO BOX 200 WODEN ACT 2606 AUSTRALIA Facsimile No.: (06) 285 3929	Authorized officer **J. DEUIS** Telephone No.: (06) 283 2146

Form PCT/ISA/210 (second sheet) (July 1992) copyus

C (Continuation)	DOCUMENTS CONSIDERED TO BE RELEVANT	
Category*	Citation of document, with indication, where appropriate, of the relevant passages	Relevant to claim No.
X	Derwent Abstract Accession No. 91-256966/35, Class V02, JP, A, 03-167 803 (SHINETSU CHEM IND KK) 19 July 1991.	1,8
X	Derwent Abstract Accession no. 46923 E/23, Class L03 M22 P53, JP, A, 57 - 070205 (TOKYO SHIBAURA ELEC LTD) 30 April 1982.	1
X	Derwent Abstract Accession No. 88-018326/03, Class V02, JP, A, 62 - 281308 (DAIDO TOKUSHUKO KK) 7 December 1987.	1

This Annex lists the known "A" publication level patent family members relating to the patent documents cited in the above-mentioned international search report. The Australian Patent Office is in no way liable for these particulars which are merely given for the purpose of information.

Patent Document Cited in Search Report		Patent Family Member					
EP	253521	AU	75251/87	BR	8703666	CA	1275377
		CN	87104923	JP	63031102	US	4778542
DE	1262986	NL	6412895	BE	655786	CH	487076
				.			
						END OF ANNEX	